Journal of Computers Vol. 36 No. 5, October 2025, pp. 219-233
https://doi.org/10.63367/199115992025103605015

A Building Outline Regularization Method Based on U^2-Net Segmentation Results

Fei-Fei Xie, Fu-Zheng Chu*, Yu-Chao Gu, and Lin Sun

College of Geodesy and Geomatics, Shandong University of Science and Technology, Qingdao 266590, China

cfz00532024@163.com

Received 25 March 2025; Revised 14 July 2025; Accepted 4 August 2025

Abstract. In recent years, certain achievements have been made in extracting buildings from high-resolution remote sensing images using convolutional neural networks. However, the obtained building masks still have problems such as blurred boundaries and irregular shapes, which are far from the actual building boundaries. Therefore, they cannot be directly applied to many cartographic and engineering applications. In this study, a new post-processing method for building outline regularization based on convolutional neural network segmentation results is proposed. The method incorporates classical boundary regularization methods (e.g., the outer rectangle method and the Douglas-Peucker (DP) algorithm) and employs a data-driven approach in the pixel domain to regularize polygons using a priori geometric conditions. Compared with other methods on the WHU public dataset, experiments show that our algorithm is effective in improving the accuracy and regularity of building outlines, and still retains more detailed features even for complex building outline.

Keywords: high-resolution remote sensing imagery, building outline extraction, outline regularization, rectangular criterion, perceptual grouping

1 Introduction

Generating building profile vectors from high-resolution remote sensing images has received increasing attention in recent years due to its wide range of applications in urban planning, smart city development, and cartographic mapping [1-4]. Accurately extracting vectorized building outlines from complex urban scenes is essential for achieving high-quality geospatial data products. However, this task remains challenging due to the diversity of building materials and architectural forms, as well as the variations in illumination, occlusion, and background noise inherent in remote sensing imagery [5].

One of the major technical difficulties lies in the complexity of roof structures and the irregularity of building contours. Traditional methods often rely on handcrafted features or rule-based segmentation. However, these methods typically fail to generalize well to complex urban scenes. With the rapid advancement of deep learning, pixel-level building segmentation techniques have demonstrated superior performance over manual feature engineering approaches, enabling more accurate and automated extraction of building regions. However, despite their high per-pixel classification accuracy, the resulting building boundaries are often fuzzy and irregular, lacking clear geometric consistency due to the absence of structural constraints in conventional segmentation networks.

To solve the above challenges, two main solution paradigms currently prevail. The first is end-to-end deep learning models that integrate building segmentation and polygonal outline regularization into a unified framework. Representative models include contour-based networks (DARNet [6], ACDRNet [7]), graph convolutional network (GCN [8], Deep Snake [9]), and RNN-based methods (PolyMapper [10], HiSup [11]). These methods aim to directly predict vectorized building shapes by learning from annotated masks. However, such approaches heavily rely on the quality of the predicted masks, which often contain edge ambiguity and shape distortions. This ambiguity hinders accurate polygon reconstruction, and in practice, the gap between predicted polygon quality and ground-truth annotations remains significant. Some recent works attempted to mitigate this by introducing structural priors, such as Frame-Field [12] or improved the polygonal mapping of buildings schemes [13] with the off-the-shelf mask predictions, but challenges such as shape reversibility and structural consistency persist.

* Corresponding Author

The second paradigm involves a two-step strategy, where deep networks are first used for semantic segmentation of buildings, followed by geometric post-processing to regularize the extracted outlines. This approach decouples segmentation from regularization, allowing more flexible incorporation of prior knowledge. For example MA- FCN-based segmentation +Douglas-Peucker regularization [14], Mask R-CNN with building boundary regularization [15]. Among post-processing strategies, current regularization techniques can be categorized into three main types: firstly, methods based on image morphological processing. secondly, regularization methods assisted by point cloud data. thirdly, methods using image feature information. The methods using image morphological processing are mainly based on morphological processing(erosion, expansion, etc.) of high-resolution images of building outlines to make morphological corrections to the outlines [16]. In contrast, outline regularization methods assisted by laser point cloud data typically utilize the elevation information provided by the point cloud to enhance the geometric accuracy of building outlines and remain a major focus in current research on outline regularization [17-19]. However, these methods are inherently dependent on the availability and quality of 3D point cloud data, which often has limited spatial coverage and may not be available for all remote sensing scenarios, thereby restricting their general applicability. Alternatively, outline regularization methods based on image feature information aim to reconstruct building outlines by extracting and aligning geometric primitives such as straight lines [20, 21], corner points [22, 23] , and minimum external rectangles [24]. Although these methods are more data-accessible and computationally efficient, they often suffer from geometric incompleteness and lack the ability to preserve fine structural details. For example, the Hough transform is prone to miss detection of short edges, corner points being obscured or blurred, and other causes of corner point matching and extraction errors.

Motivated by these limitations, this study proposes a novel building outline regularization method that leverages pixel-wise deep segmentation results and incorporates geometric priors in the post-processing stage. Based on DP algorithm for polygon simplification [25], the algorithm is able to effectively approximate the original curve as a simplified curve composed of a few keys. On this basis, we further design two strategies for the precise correction and adjustment of contour segments, converting the segmented building outlines into regularized vector boundaries. Experimental results on the WHU public building dataset demonstrate that the proposed method significantly enhances the accuracy and regularity of building outlines. Even when dealing with complex building shapes, it effectively preserves fine-grained structural details and geometric features. In summary, the main contributions of this study are as follows:

(1) A post-processing method for building outline regularization is proposed based on CNN segmentation results, which effectively enhances the regularity and applicability of building boundaries by leveraging geometric priors in the pixel domain.
(2) Two contour correction and adjustment strategies are introduced based on the traditional Douglas-Peucker (DP) algorithm, enabling the transformation of raw segmentation contours into regularized vector boundaries while preserving architectural details.
(3) Extensive experiments on the WHU public building dataset demonstrate the superiority of the proposed method in terms of outline accuracy and regularity, particularly in retaining more detailed features for complex building shapes.

The main contents of this paper are as follows: Section 2 introduces the process and principle of the algorithm in detail; Section 3 is the experiment and analysis, and Section 4 is a summary of the whole paper.

2 Methodology

Our proposed method is divided into three modules (Fig. 1): polygon simplification, regularization based on the rectangular criterion, and regularization based on the perceptual grouping algorithm. First, based on the building segmentation results, the DP algorithm is used to simplify the outline, achieving preprocessing of the building outline. Then, the optimal bounding rectangle of the building is determined according to its dominant direction. For small buildings, the optimal bounding rectangle is used to replace the original outline, while for large buildings, the optimal bounding rectangle combined with Hausdorff distance is used to correct part of the outline, achieving initial regularization. Finally, angle constraints are employed to group unprocessed boundary points. For each group, the least squares method is used to fit lines, and the locations of boundary points are used to estimate line segments. Spurious or noisy line segments are removed based on their dominant direction and neighborhood relationships. A perceptual grouping strategy is then applied to connect and reconstruct the remaining line segments, ensuring the resulting building boundaries are both accurate and regularized.

2.1 Polygon Simplification

Based on the geometric properties of buildings, we use perimeter (4.5m) and area (1.44m²) thresholds to filter out small structures and pixel classification noise. Using the segmentation results of the binarized buildings (Fig. 2(a)), we extract building outlines by tracking closed regions in the binary map (Fig. 2(b)). However, the extracted contours often contain a large number of redundant vertices, making the raw contour edges unsuitable for further processing. Removing these redundant points helps reduce data complexity without altering the overall geometric shape of the buildings. Therefore, in the subsequent steps, we apply polygon simplification to reduce the data size while preserving essential structural features. To preserve geometric detail, we carefully select a threshold for contour simplification. A large threshold in the Douglas–Peucker (DP) algorithm may overly smooth the boundaries, causing loss of critical features. In contrast, a small threshold results in minimal simplification, leaving redundant points. To balance these factors, we use a relatively small simplification threshold (0.5m), ensuring that key contour features are preserved while reducing the number of vertices. Additionally, we iteratively simplify the contours during the optimization process, gradually refining the shape until the optimal result is achieved. The number of vertices before and after simplification is shown in Fig. 2(c) and 2(d), demonstrating that this method effectively removes redundant points while maintaining the detailed characteristics of the building outlines.

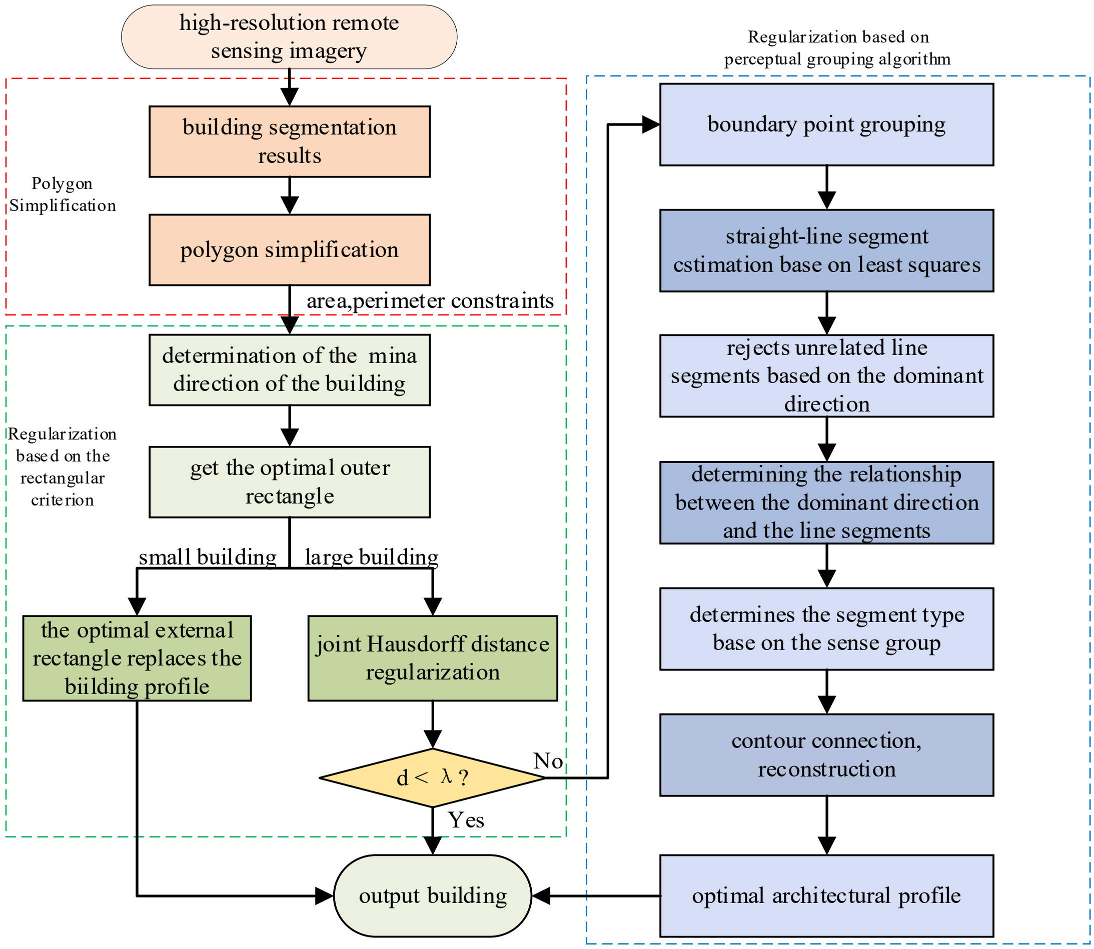

Fig. 1. Building outline regularization flow chart

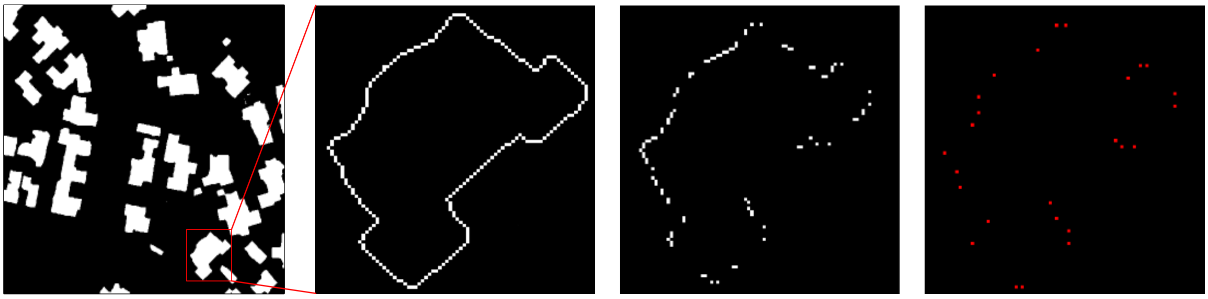

(a) (b) (c) (d)

(a) Results of the division (b) Outline tracking results (c) Key points of the building boundary (d) Simplified DP algorithm effect

Fig. 2. Comparison of simplified effects of the boundary points

2.2 Regularization Based on the Rectangular Criterion

Due to boundary ambiguity and irregular shapes in coarse building segmentation results, polygons generated by the Douglas–Peucker (DP) algorithm often fail to correct certain errors—such as corners that should be right angles, or straight edges that are fragmented into multiple line segments. In order to reduce this error, we introduce the rectangle criterion to regularize the outline [26]. To improve the performance of the minimum enclosing rectangle algorithm, we propose a method to determine the optimal enclosing rectangle based on the main direction of any building, which is called the voting and rotating caliper algorithm. Finally, we incorporate the Hausdorff distance algorithm [27], using the unidirectional distance between the simplified polygon and the fitted rectangle as a criterion to assess the suitability of the final outline. The specific steps are as follows:

a) Preliminary estimation of the main direction of the building. Let the set of line segments consisting of the fitted polygons of the building outline be $L = \{l_1, l_2, \ldots, l_n\}$, without distinguishing between the starting and ending points of the line segments, and calculate the angle between each line segment and the horizontal direction, denoted as $A = \{a_1, a_2, \ldots, a_n\}$, then $\in [0,180)$. The length of each line segment is denoted as $Len(l_i)$, and then the number of votes of that line segment is $w_i = \frac{Len(l_i)}{\Sigma_{t=1}^{n} Len(l_t)}$. A two-dimensional accumulator array is created with the weight of the length of each line segment, the interval da (taken as 10° in this paper), and the peak a_m in the array is the general direction of the building (Fig. 3).

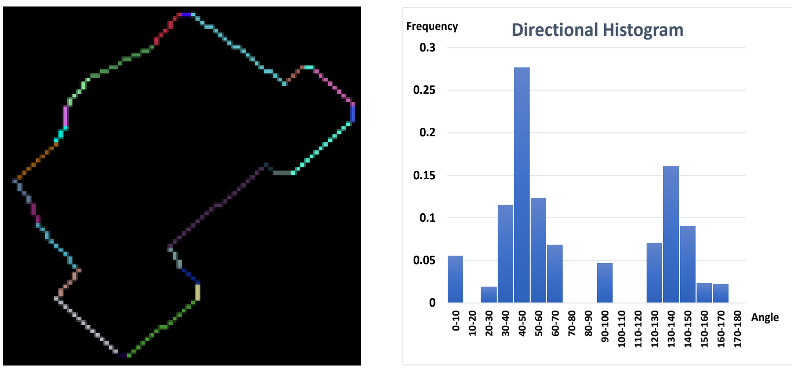

(a) (b)

(a) Segment information (b) Histogram of line segment directions

Fig. 3. Building outline regularization flow chart

b) The rotating caliper algorithm determines the optimal external rectangle and main direction. The external rectangle of the building outline at each rotation angle is found in 1° rotation steps within the angle [a_{main}-da, a_{main}+da] (Fig. 4(a)), and the external rectangle with the smallest area is taken as the optimal external rectangle (Fig. 4(b)), where the main building direction is the angle value corresponding to the long side of this rectangle.

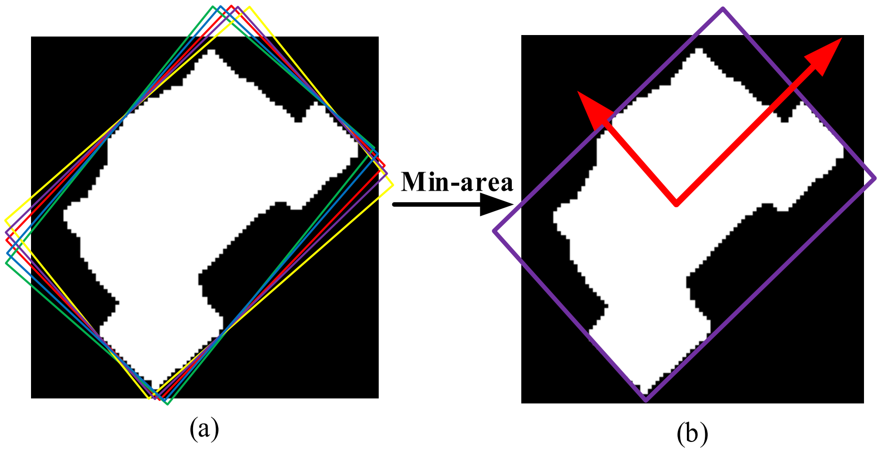

(a) External rectangles at different rotation angles (b) Optimal external rectangle and main direction

Fig. 4. Determination of the optimal external rectangle

c) Joint Hausdorff distance correction of the optimal external rectangle. The fitted polygonal outline of the building is divided into equal-length segments (Fig. 5(a)). For each segment, we compute the one-way Hausdorff distance to the corresponding side of the optimal external rectangle. If the distance is below a predefined threshold, it suggests that the segment closely matches a portion of the rectangle's outline. If a segment satisfies this condition, its coordinates are replaced by the corresponding side of the rectangle. Otherwise, the original coordinates are retained (Fig. 5(b)). This procedure produces the initial regularization result for the building outline (Fig. 5(c)).

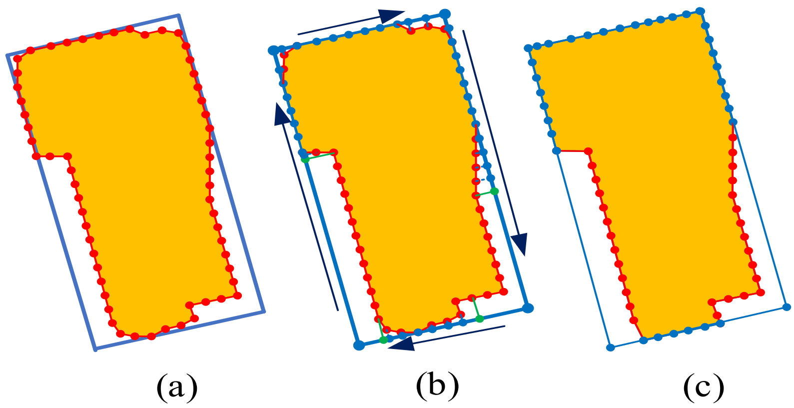

(a) The set of line segments is divided into equal parts (b) Similarity calculations (c) Regularized result

Fig. 5. Schematic of the outline regularization of the Hausdorff distance algorithm

Buildings are classified into two categories based on geometric size: those with a perimeter under 24 m and an area below 44 m² are considered small, while all others are regarded as large. Small buildings, which typically exhibit simple rectangular shapes, are directly replaced with their optimal minimum bounding rectangles.

For large buildings, we apply the one-way Hausdorff distance with a threshold of 0.9 to determine whether each polygon edge should be replaced by the corresponding segment of the rectangle. The regularization results using the rectangular criterion are presented in Fig. 6, where (a) is the optimal outer rectangle for each building, and (b) is the result of outline regularization through the optimal outer rectangle. In blue is the result of regularizing simple and small buildings by the optimal outer rectangle, and in green is a partial outline of a complex building regularized by the optimal outer rectangle and the Hausdorff distance. It can be seen that the optimal outer rectangle replaces the original small, simple building, eliminating the shading effect, and the shape becomes a regular rectangular structure; for the complex building, the outlines of the outer edges of the building are effectively regularized.

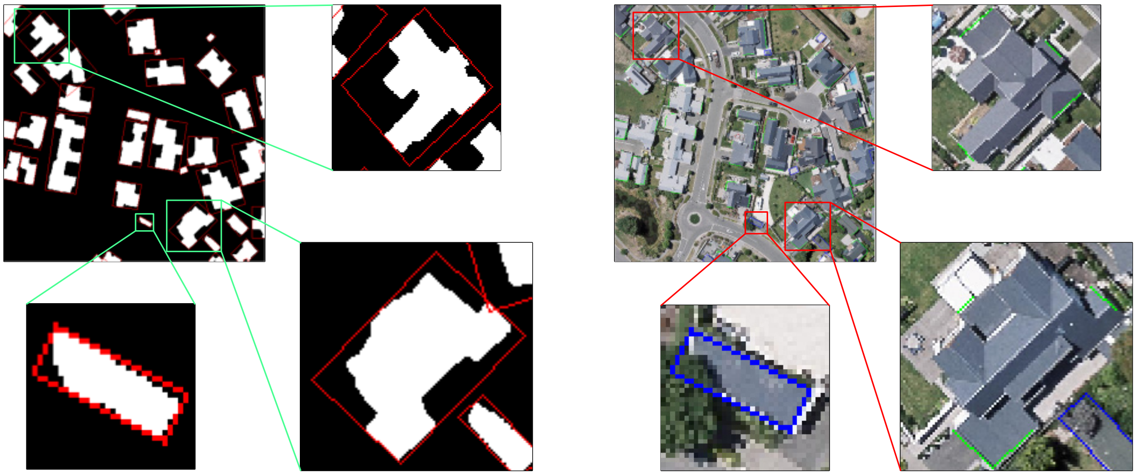

(a) (b)

(a) Optimal external rectangle (b) Regularized result

Fig. 6. Outline of regularization rendering

2.3 Regularization Based on Perceptual Grouping Algorithm

We propose a method for subsequent regularization using a combination of outline vertices, least-squares straight-line fitting, and perceptual grouping [28]. Specifically, we first group the outline vertices and then apply least-squares fitting to extract straight line segments. This approach helps preserve detailed geometric features of the buildings. However, it may introduce an excessive number of short, overlapping segments. To prevent too many straight lines from intersecting confusingly and causing difficulties in solving between line segments, we suppressed the length of the straight lines to obtain boundary line segments that are consistent with the shape of the building. The specific steps are as follows:

a) Using the main direction constraint to eliminate the wrong line segment. To better preserve the building's right-angle features, we assess each segment based on its angular relationship with the dominant building orientation. Due to occlusion or image blur, building corners may deviate from ideal right angles, making some segments unreliable. If a line segment has no possibility of being parallel or perpendicular to the main building direction, and the length of the line segment is very short, we consider the line segment to be an error line segment (Fig. 7(b)).

b) Line segment tracing using proximity constraints. To prevent incorrect connections between line segments, it is necessary to ensure that the endpoints (starting points) of a given line segment can only be connected to the starting points (endpoints) of neighboring line segments, for which a line segment chain can be constructed using the proximity constraint criterion (Fig. 7(a)). Specifically, for each segment endpoint, we compute its distances to the endpoints of all other segments and identify the nearest one as its connection candidate. By iteratively linking segments based on this proximity rule, a continuous line segment chain is formed until all endpoints are connected.

c) Straight line grouping. The line segments that are perpendicular and parallel to the main building direction and longer line segments are retained by step 1), and the line segment chain constructed by step 2) enables relationships to be established between the line segments. Based on the line segment information, the inter-adjacent line segments can be classified into intersecting and diverging relationships. Let the angle threshold be ta. When the angle between two line segments is less than the threshold ta, the two line segments are parallel (Fig. 7(c)); when the angle between two line segments is greater than the threshold ta, the two line segments are intersecting (Fig. 7(d)).

For intersecting line segments, the intersection point of the two line segments can be found using the linear formula where the line segments are located instead of the part of the two line segments that are connected. Let the coordinates of the endpoints of one line segment $A(x_1, y_1)$, $B(x_2, y_2)$ and the coordinates of the endpoints of the other line segment $C(x_3, y_3)$, $D(x_4, y_4)$, the equation of the line is

$$A_1x + B_1y + C_1 = 0 \tag{1}$$

$$A_2x + B_2y + C_2 = 0 \tag{2}$$

$$A_1 = y_2 - y_1,\ B_1 = x_1 - x_2,\ C_1 = x_2y_1 - x_1y_2. \tag{3}$$

$$A_2 = y_4 - y_3,\ B_2 = x_4 - x_3,\ C_2 = x_4y_3 - x_3y_4. \tag{4}$$

The system of joint cubic equations yields:

$$x = \frac{B_1C_2 - B_2C_1}{A_1B_2 - A_2B_1}, y = \frac{A_2C_1 - A_1C_2}{A_1B_2 - A_2B_1}. \tag{5}$$

For the separated line segments, the distance constraint is used to determine whether the two line segments are on the same line. Let the distance threshold *td*, when the Euclidean distance of the neighboring endpoints of two line segments is less than the threshold *td*, then the two line segments can be considered to be approximately on the same line, then the two line segments can be merged into one line segment; when the distance is greater than the threshold *td*, then the two line segments are not considered to be on the same line, then the angle value and endpoint coordinates of one line segment are used to construct a vertical line segment, let the endpoint of l_2 adjacent to line segment l_1 is $M(x_m, y_m)$, the equation of the line where l_1 and l_2 are located is

$$A_3x + B_3y + C_3 = 0. \tag{6}$$

$$A_4x + B_4y + C_4 = 0. \tag{7}$$

Subsequently the equation of the line passing through the point M and perpendicular to l_1 is

$$B_3x - A_3y + \left(A_3y_m - B_3x_m\right) = 0 \tag{8}$$

The system of joint equations gives the coordinates of the other end of the vertical line segment as

$$x = \frac{B_4\left(B_3x_m - A_3y_m\right) - A_3C_4}{A_3A_4 + B_3B_4}, y = \frac{A_4\left(A_3y_m - B_3x_m\right) - B_3C_4}{A_3A_4 + B_3B_4}. \tag{9}$$

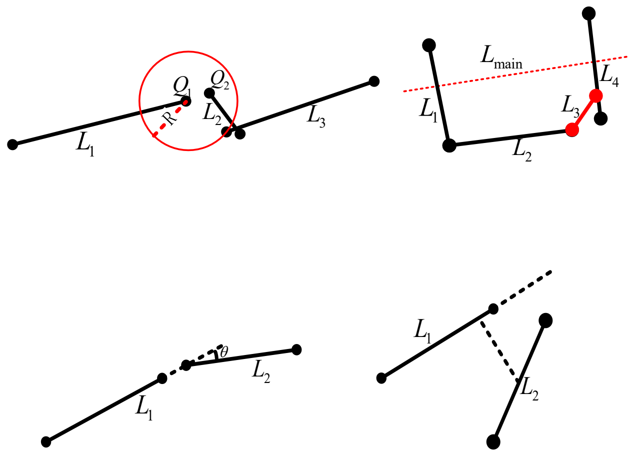

(a) Proximity constraints (b) Principal direction constraint (c) Angle constraints (d) Side distance constraints

Fig. 7. Segment relationship

We set the threshold $\alpha = \frac{\pi}{9}$ for grouping boundary points, and after fitting straight lines to the boundary points, we use the principal direction angle constraint threshold $\beta = \frac{\alpha}{2}$ and the line segment length l=0.4m to reject the wrong line segments, and the principal direction distance constraint d=2m to determine whether to construct new line segments to connect parallel line segments. The regularization results using perceptual grouping are given in Fig. 8, where (b) shows the optimal external rectangles for each building, and (b) is a plot of the results of outline regularization through the optimal external rectangles. In Fig. 8(d), the blue shows the result of regularizing simple, small buildings using the optimal bounding rectangle, while the green shows the result of regularizing the complex building outlines using the optimal bounding rectangle combined with Hausdorff distance. For small buildings, the optimal rectangle eliminates the influence of vegetation shading and yields a regular rectangular shape. For complex structures, the combined method effectively preserves key contours while improving geometric regularity.

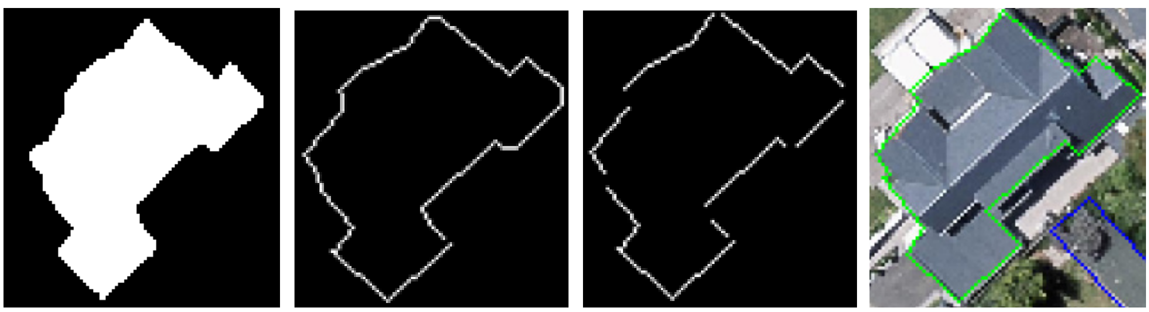

(a) (b) (c) (d)

(a) Splitting result (b) Line segment results (c) Segment culling (d) Perception grouping results

Fig. 8. Perceptual grouping of straight line segments

3 Experimental Method and Analysis

3.1 Data Set and Parameter Settings

The data used in this study is WHU data (http:// study.rsgis.whu.edu.cn/pages/download/), including a 450 km^2 aerial image of Christchurch, New Zealand. The data contains approximately 22,000 individual buildings with spatial resolution of 0.075m, which was subsequently down sampled to 0.3m.

We implemented image segmentation and building extraction using deep learning methods [29]. The model uses the Adam optimizer with hyperparameters set to default values (initial learning rate lr =10-3, betas=(0.9,0.999), eps=10-8, and weight decay weight decay=0). The data is divided into training set (4736 images), test set (2416 images) and validation set (1036 images).

3.2 Evaluation Metrics

To quantify the accuracy of building outlines before and after regularization, the four most commonly used evaluation metrics: correctness (CR), completeness (CM), integrated value (F1), and overall accuracy (OA), were evaluated [30]. Moreover, the manually selected real reference results were compared with the extracted results, and the accuracy from a pixel-based and object-based perspectives was evaluated.

$$V_{CR} = \frac{|V_{TP}|}{|V_{TP}|+|V_{FP}|}, V_{CM} = \frac{|V_{TP}|}{|V_{TP}|+|V_{FN}|}, F_1 = \frac{2V_{CR}\times V_{CM}}{V_{CR}+V_{CM}}, V_{OA} = \frac{|V_{TP}|}{|V_{TP}|+|V_{FP}|+|V_{FN}|}. \tag{10}$$

where: $|V_{TP}|$ is the number of pixels or objects judged as buildings; $|V_{FP}|$ is the number of pixels or objects judged as buildings for non-buildings; $|V_{TN}|$ is the number of pixels or objects judged as non-buildings for non-buildings.

3.3 Building Outline Regularization Experiments

Experiment 1: The building outline extraction scheme in this paper is experimentally compared with the HiSup method [11], which uses an end-to-end building vector edge regularization method based on deep learning.

We conducted experimental verification on a validation set consisting of 1,036 images. To demonstrate the feasibility of the method, we visualized the outline extraction results for two representative types of buildings. Type 1 represents low to medium density building areas partially obstructed by vegetation, while Type 2 consists of dense building clusters guided by the road network. The outline extraction results for Type 1 and Type 2 using the HiSup method are shown in Fig. 9(a) and Fig. 10(a), respectively, while the results of the proposed method are shown in Fig. 9(c) and Fig. 10(c). From the result images, we observed that the HiSup method exhibits multiple inaccuracies in outline extraction in both images (the blue boxes in Fig. 9(a) and Fig. 10(a)). Additionally, when buildings are shaded by features with similar colors to surrounding non-building areas or trees, the method is more prone to misdetection (the red boxes in Fig. 9(a) and Fig. 10(a)). When building density is high, multiple buildings are misclassified as a single building (the yellow box in Fig. 10(a)). Buildings detected using U^2-Net rarely show misclassification or omission, though buildings shaded by trees may still have some missing (the red box in Fig. 9(b)), while the boundaries of complex buildings tend to be blurred and irregular (the blue box in Fig. 9(b)). Regarding regularization performance, HiSup tends to produce overly simplified linear outlines that fail to preserve architectural detail. Our proposed regularization algorithm, however, consistently generates more accurate and geometrically coherent building contours, regardless of scale or complexity.

Experiment2: Based on the results of U^2-Net segmentation, in order to further highlight the feasibility of the proposed method, the regularization method in this paper is compared with the regularization tool of ArcGIS Pro software [31], the method based on the smallest circumscribed rectangle [32], and the method based on angle detection [33].

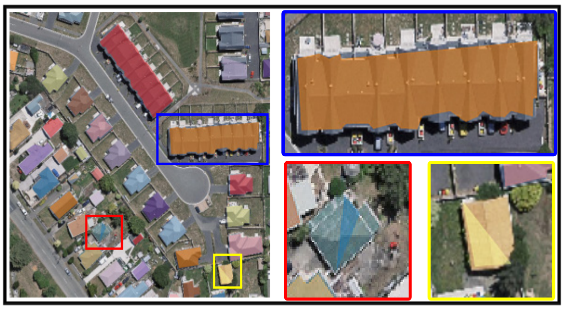

(a) HiSup method

(b) U2-Net Segmentation Results

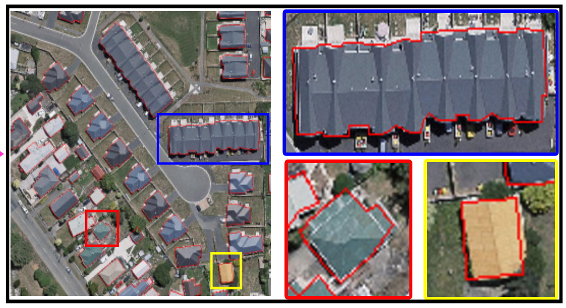

(c) Our method

Fig. 9. Building outline extraction results for Type 1 buildings with different solutions

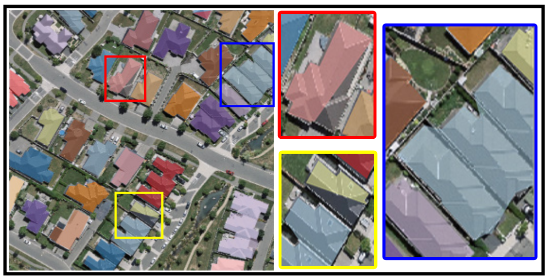

(a) HiSup method

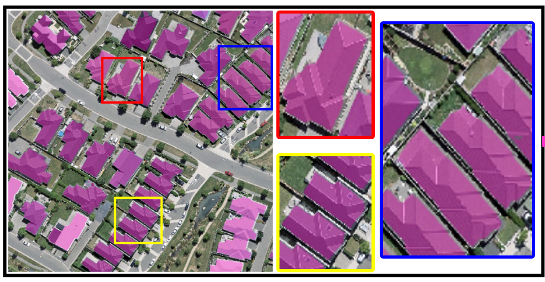

(b)U2-Net Segmentation Results

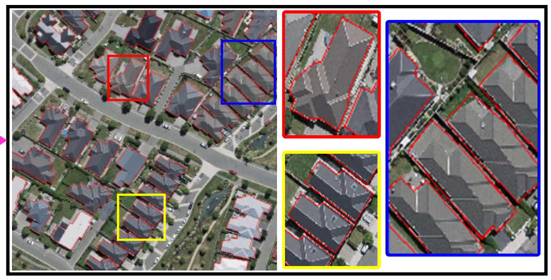

(c) Our method

Fig. 10. Building outline extraction results for Type 2 buildings with different solutions

Fig. 11 and Fig. 12 present the outline extraction results for Type 1 and Type 2 buildings using different regularization methods. Due to the complexity and integrity of building outline, different methods exhibit varying levels of effectiveness in processing these outlines.

First, ArcGIS Pro software has certain limitations when handling complex building areas, particularly when building structures are intricate or outline information is missing (blue box in Fig. 11(a) and red box in Fig. 12(a)). Due to occlusions or incomplete data, some building outline information cannot be accurately extracted, causing the software to regularize the obscured areas back to the original shape of the building rather than the actual outline (red box in Fig. 11(a) and yellow box in Fig. 12(a)). This phenomenon leads to a loss of local details in the outlines and affects the precision of building boundary representation.

Second, the minimum bounding rectangle method tends to cause outward expansion when there are many curves in the outer outlines (blue box in Fig. 11(b)). Although this method provides an overall outline fitting approach, it struggles to handle concave areas or missing sections. When a building's outline is significantly incomplete, this method fails to maintain its original shape, resulting in blurred boundaries and irregular forms (red and yellow boxes in Fig. 11(b), red box in Fig. 12(b)). Additionally, this method has limitations in processing building corners, making it difficult to preserve the turning features of structures, which affects the realistic representation of building outlines.

Third, the corner detection method suffers from inaccurate corner point selection when building outlines are occluded or corner points are missing, which negatively impacts the reconstruction of the outlines. Due to the imprecise selection of corner points, this method is less effective in filling in missing sections. Furthermore, it often directly connects the detected corner points to restore building outlines, but this strategy may lead to the loss of small corner details, producing overly smooth outlines that lack the fine details of the original building (Fig. 11(c) and 12(c)).

In contrast, our method performs significantly better in restoring missing outline sections and effectively complements building boundary information while maintaining high accuracy in complex building scenarios. Our method not only corrects blurry boundaries but also preserves fine building details, avoiding the distortion issues found in traditional methods when dealing with complex outlines. By implementing optimized regularization strategies, our approach achieves a more comprehensive restoration of the original building shape, enhances the accuracy of outline representation, and ultimately delivers superior regularization results, as shown in Fig. 11(d) and 12(d).

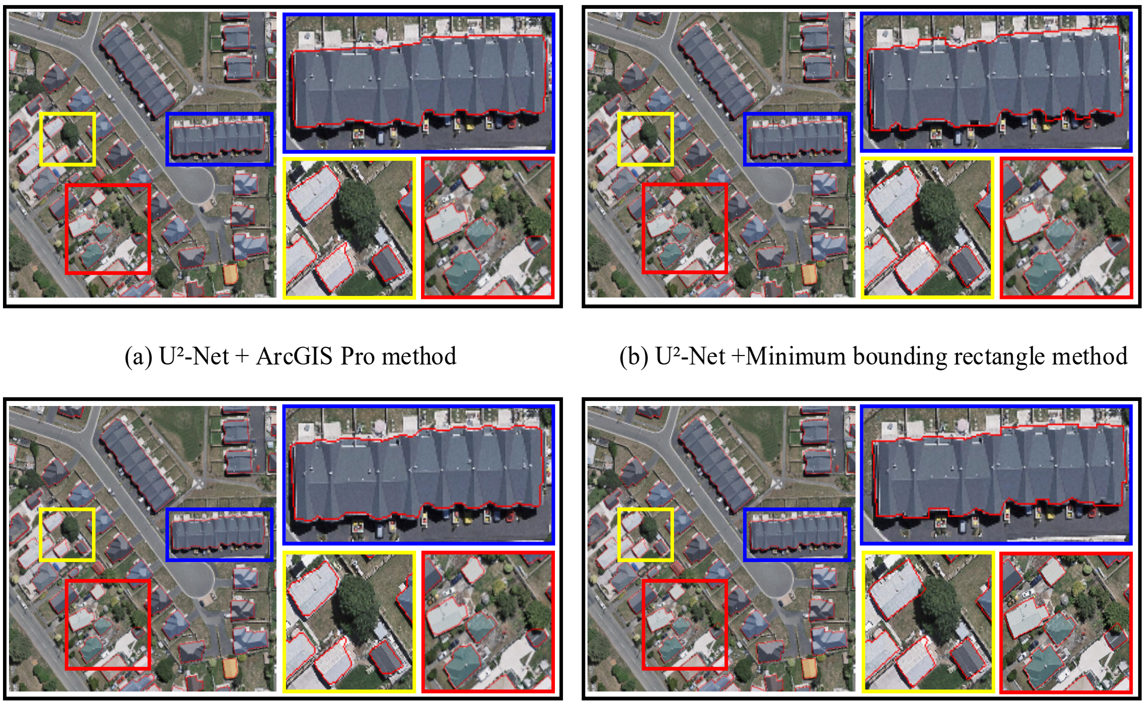

(a) U²-Net + ArcGIS Pro method

(b) U²-Net +Minimum bounding rectangle method

(c) U²-Net + Corner point detection method

(d) U²-Net + Our method

Fig. 11. Contour extraction results for Type 1 buildings using different regularization methods

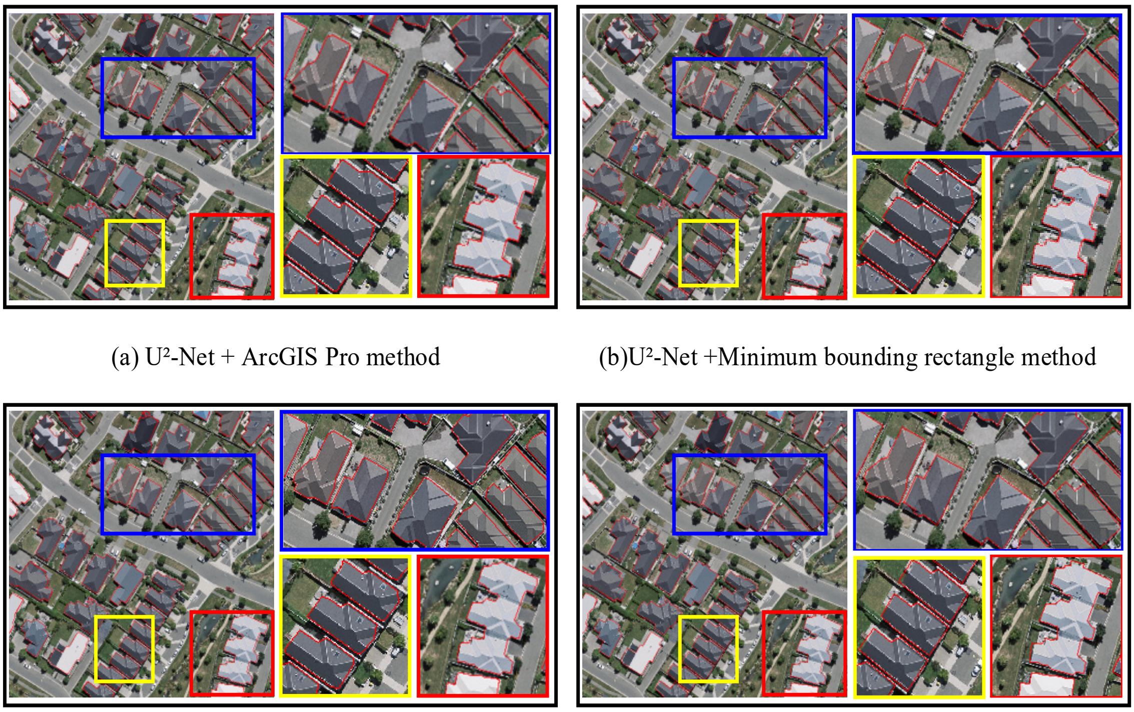

(a) U²-Net + ArcGIS Pro method (b)U²-Net +Minimum bounding rectangle method

(c) U²-Net + Corner point detection method (d) U²-Net + Our method

Fig. 12. Contour extraction results for Type 2 buildings using different regularization methods

To provide a comprehensive evaluation of our method, we selected 50 images each from two representative building areas: Type 1, low to medium density building areas partially obscured by vegetation, and Type 2, dense building clusters guided by road networks, for quantitative assessment. We then calculated the average values of the evaluation metrics for these samples. The comparison of the average accuracy of building contour regularization for the two types of buildings is presented in Table 1. The combined value of our method improved by 1.27% and 1.96%, respectively, and the overall accuracy improved by 0.42% and 1.41%, compared to the initial detection results. These improvements demonstrate the effectiveness of our method, with both the combined value and overall accuracy achieving notable gains that surpass traditional benchmarks. More importantly, our method can improve the completeness and regularity of the building inspection results.

Table 1. Comparison of building regularization results

Image class	The type of algorithm	Method name	CM	CR	F1	OA
Type 1	End-to-end	HiSup method	85.32	83.91	84.61	87.27
	U²-Net segmentation+ post-processing	ArcGIS Pro method	91.03	92.37	91.70	89.34
		Minimum bounding rectangle method	90.97	92.41	91.68	89.37
		Corner point detection method	90.89	92.36	91.62	89.29
		Our method	**91.97**	**93.54**	**92.75**	**89.63**
Type 2	End-to-end	HiSup method	84.86	79.25	81.96	83.54
	U²-Net segmentation+ post-processing	ArcGIS Pro method	90.03	91.17	90.60	89.43
		Minimum bounding rectangle method	90.97	91.83	90.78	89.46
		Corner point detection method	90.19	91.38	90.78	89.46
		Our method	92.03	92.47	92.25	90.68

4 Conclusion

End-to-end building edge extraction networks are considered an automated AI application, but combining deep feature learning networks with heuristic design may be more practical. We propose a post-processing method for regularizing building outline polygons based on prior geometric conditions. First, the building segmentation results are used to generate initial polygons using the DP algorithm as a preprocessing step. Then, building contour information was used to construct a minimum external rectangle that conforms to the main building direction, allowing the regularization of the contours for the first time. Finally, a constraint model was constructed based on the estimation results of the boundary straight segments to connect and reconstruct the straight segments using prior knowledge. Experimental results show that our method achieves an average overall accuracy of 90.16% for different types of building areas, representing a significant improvement compared to deep learning methods. It also shows some improvement over post-processing methods such as the ArcGIS Pro method, Minimum bounding rectangle method, and Corner point detection method. However, our method preserves the details of building contours and restores occluded building geometries without damaging the original structure. By fine-tuning the contours based on building detection results, it makes the building extraction results more regularized and improves consistency with the actual building shapes, offering potential improvements for current building extraction post-processing tasks.

To address the issue of severe occlusion in initial detection results, we plan to incorporate raw image information (e.g., color and texture features) into future regularization work. Additionally, we will apply curve fitting to the rounded corners of buildings to enhance the algorithm's applicability in handling non-right-angled structures.

5 Acknowledgement

This work is supported by Shandong Provincial Natural Science Foundation Project (ZR2021MD026).

References

[1] J. Song, J. Wu, Y. Jiang, Extraction and reconstruction of curved surface buildings by contour clustering using airborne LiDAR data, Optik 126(5)(2015) 513-521.
https://doi.org/10.1016/j.ijleo.2015.01.011

[2] Q. Chen, L. Wang, S.L. Waslander, X. Liu, An end-to-end shape modeling framework for vectorized building outline generation from aerial images, Isprs Journal of Photogrammetry and Remote Sensing 170(2020) 114-126.
https://doi.org/10.1016/j.isprsjprs.2020.10.008

[3] D. Zheng, J. Kang, K. Wu, Y. Feng, H. Guo, X. Zheng, S. Li, F. Fang, Semi-Supervised Building Detection from High-Resolution Remote Sensing Imagery, Sustainability 15(15)(2023) 11789.
https://doi.org/10.3390/su151511789

[4] S. Wei, T. Zhang, D. Yu, S. Ji, Y. Zhang, J. Gong, From lines to Polygons: Polygonal building contour extraction from High-Resolution remote sensing imagery, Isprs Journal of Photogrammetry and Remote Sensing 209(2024) 213-232.
https://doi.org/10.1016/j.isprsjprs.2024.02.001

[5] W. Zhao, C. Persello, A. Stein, Building outline delineation: From aerial images to polygons with an improved end-to-end learning framework, Isprs Journal of Photogrammetry and Remote Sensing 175(2021) 119-131.
https://doi.org/10.1016/j.isprsjprs.2021.02.014

[6] D. Cheng, R. Liao, S. Fidler, R. Urtasun, DARNet: Deep Active Ray Network for Building Segmentation, in: Proc. IEEE Conference on Computer Vision and Pattern Recognition (CVPR), 2019.
https://doi.org/10.1109/CVPR.2019.00761

[7] S. Gur, T. Shaharabany, L. Wolf, End to end trainable active contours via differentiable rendering. <https://arxiv.org/abs/1912.00367>, 2019 (accessed 15.01.2025).

[8] S. Wei, S. Ji, Graph Convolutional Networks for the Automated Production of Building Vector Maps From Aerial Images, IEEE Transactions on Geoscience and Remote Sensing 60(2022) 5602411.
https://doi.org/10.1109/TGRS.2021.3060770

[9] S.D. Peng, W. Jiang, H.J. Pi, X.L. Li, H.J. Bao, X.W. Zhou, Deep Snake for Real-Time Instance Segmentation, in: Proc. IEEE/CVF Conference on Computer Vision and Pattern Recognition (CVPR), 2020.
https://doi.org/10.1109/CVPR42600.2020.00856

[10] Z. Li, J.D. Wegner, A. Lucchi, Topological Map Extraction From Overhead Images, in: Proc. IEEE/CVF International Conference on Computer Vision (ICCV), 2019.

https://doi.org/10.1109/ICCV.2019.00180
[11] B. Xu, J. Xu, N. Xue, G.-S. Xia, HiSup: Accurate polygonal mapping of buildings in satellite imagery with hierarchical supervision, Isprs Journal of Photogrammetry and Remote Sensing 198(2023) 284-296.
https://doi.org/10.1016/j.isprsjprs.2023.03.006
[12] N. Girard, D. Smirnov, J. Solomon, Y. Tarabalka, Polygonal Building Extraction by Frame Field Learning, in: Proc. IEEE/CVF Conference on Computer Vision and Pattern Recognition (CVPR), 2021.
https://doi.org/10.1109/CVPR46437.2021.00583
[13] M. Li, F. Lafarge, R. Marlet, Approximating shapes in images with low-complexity polygons, in: Proc. IEEE/CVF Conference on Computer Vision and Pattern Recognition (CVPR), 2020.
https://doi.org/10.1109/CVPR42600.2020.00866
[14] S. Wei, S. Ji, M. Lu, Toward Automatic Building Footprint Delineation From Aerial Images Using CNN and Regularization, IEEE Transactions on Geoscience and Remote Sensing 58(3)(2020) 2178-2189.
https://doi.org/10.1109/TGRS.2019.2954461
[15] K. Zha, J. Kang, J. Jung, G. Sohn, Building Extraction from Satellite Images Using Mask R-CNN with Building Boundary Regularization, in: Proc. IEEE/CVF Conference on Computer Vision and Pattern Recognition (CVPR), 2018.
https://doi.org/10.1109/CVPRW.2018.00045
[16] W. Wang, J. Du, X. Li, H. Hu, W. Xu, H. Guo, Y. Ding, A Grid Filling Based Rectangular Building Outlines Regularization Method, Geomatics and Information Science of Wuhan University 43(2)(2018) 318-324.
https://dx.doi.org/10.13203/j.whugis20160071
[17] S.A.N. Gilani, M. Awrangjeb, G. Lu, An Automatic Building Extraction and Regularisation Technique Using LiDAR Point Cloud Data and Orthoimage, Remote Sensing 8(3)(2016) 258.
https://doi.org/10.3390/rs8030258
[18] J. Huang, X. Zhang, Q. Xin, Y. Sun, P. Zhang, Automatic building extraction from high-resolution aerial images and LiDAR data using gated residual refinement network, Isprs Journal of Photogrammetry and Remote Sensing 151(2019) 91-105.
https://doi.org/10.1016/j.isprsjprs.2019.02.019
[19] E. Widyaningrum, B. Gorte, R. Lindenbergh, Automatic Building Outline Extraction from ALS Point Clouds by Ordered Points Aided Hough Transform, Remote Sensing 11(14)(2019) 1727.
https://doi.org/10.3390/rs11141727
[20] T. Partovi, R. Bahmanyar, T. Krauss, P. Reinartz, Building Outline Extraction Using a Heuristic Approach Based on Generalization of Line Segments, IEEE Journal of Selected Topics in Applied Earth Observations and Remote Sensing 10(3)(2017) 933-947.
https://doi.org/10.1109/JSTARS.2016.2611861
[21] X. Zhang, T. Ai, J. Stoter, M.-J. Kraak, M. Molenaar, Building pattern recognition in topographic data: examples on collinear and curvilinear alignments, Geoinformatica 17(1)(2013) 1-33.
https://doi.org/10.1007/s10707-011-0146-3
[22] N.A. Sheik, P. Veelaert, G. Deruyter, Registration of Building Scan with IFC-Based BIM Using the Corner Points, Remote Sensing 14(20)(2022) 5271.
https://doi.org/10.3390/rs14205271
[23] X. Wang, B. Xu, S. Zhao, X. Li, Automatic registration of optical image and airborne LiDAR data based on centers and corner points of building boundaries, International Journal of Remote Sensing 43(18)(2022) 6644-6668.
https://doi.org/10.1080/01431161.2022.2142487
[24] Q. Li, A Geometric Framework for Rectangular Shape Detection, IEEE Transactions on Image Processing 23(9)(2014) 4139-4149.
https://doi.org/10.1109/TIP.2014.2343456
[25] D.H. Douglas, T.K. Peucker, Algorithms for the reduction of the number of points required to represent a digitized line or its caricature, Cartographica: the international journal for geographic information and geovisualization 10(2)(1973) 112-122.
https://doi.org/10.3138/FM57-6770-U75U-7727
[26] K.F. Lai, R.T. Chin, Deformable contours: Modeling and extraction, IEEE Transactions on pattern analysis and machine intelligence 17(11)(1995) 1084-1090.
https://doi.org/10.1109/34.473235
[27] D.P. Huttenlocher, G.A. Klanderman, W.J. Rucklidge, Comparing images using the Hausdorff distance, IEEE Transactions on pattern analysis and machine intelligence 15(9)(1993) 850-863.
https://doi.org/10.1109/34.232073
[28] K. Liu, H. Yan, K. Meng, H. Chen, H. Sajid, Iterating Tensor Voting: A Perceptual Grouping Approach for Crack Detection on EL Images, IEEE Transactions on Automation Science and Engineering 18(2)(2021) 831-839.
https://doi.org/10.1109/TASE.2020.2988314
[29] X. Qin, Z. Zhang, C. Huang, M. Dehghan, O.R. Zaiane, M. Jagersand, U^2-Net: Going deeper with nested U-structure for salient object detection, Pattern Recogn 106(2020) 107404.
https://doi.org/10.1016/j.patcog.2020.107404

[30] M. Rutzinger, F. Rottensteiner, N. Pfeifer, A comparison of evaluation techniques for building extraction from airborne laser scanning, IEEE Journal of selected topics in applied earth observations and remote sensing 2(1)(2009) 11-20. https://doi.org/10.1109/JSTARS.2009.2012488
[31] M. Pepe, D. Costantino, V.S. Alfio, G. Vozza, E. Cartellino, A novel method based on deep learning, GIS and geomatics software for building a 3D city model from VHR satellite stereo imagery, ISPRS International Journal of Geo-Information 10(10)(2021) 697.
https://doi.org/10.3390/ijgi10100697
[32] S. Wang, Y. Yang, J. Chang, X. Gao, Optimization of building contours by classifying high-resolution images, Laser & Optoelectronics Progress 57(2)(2020) 22801.
http://dx.doi.org/10.3788/LOP57.022801
[33] J.X. Wang, F. D.J. Feng, J.F. Chen, A building boundary regularization method by contrasting Harris operator and Susan operator, Bulletin of Surveying and Mapping (4)(2020) 11-15.
https://doi.org/10.13474/j.cnki.11-2246.2020.0104